ELSEVIER

0000-0000(94)00000-0

Int. J. Pres. Ves. & Piping 62 (1995) 000–000

0308-0161/95/$07.00

Propagation of stress corrosion cracks in steam generator tubes*

L. Cizelj, B. Mavko

Jožef Stefan Institute, Reactor Engineering Division, P.O. Box 100, 61111 Ljubljana, Slovenia

H. Riesch-Oppermann & A. Brücker-Foit

Kernforschungszentrum Karlsruhe, Institut für Materialforschung, P.O. Box 3640, 76021 Karlsruhe, Germany

(Received ; accepted)

Ed.?

A model suitable to describe the propagation of stress corrosion cracks in Inconel-600 made steam generator tubes is proposed in the paper. It concentrates on axial cracks located in the tube expansion transition zones which are assumed to be through-wall. The residual stress field is therefore considered as the major contributing factor driving short cracks while operational stresses dominate the growth of longer cracks. An estimate of residual hoop stresses is obtained using a non-linear finite element simulation of the tube to tube-sheet rolling process. Scatter of the residual stresses due to the stochastic variations of the dominant influencing parameters was studied. The crack propagation model utilizes linear-elastic fracture mechanics theory. In particular, both crack tips are modelled to propagate with different velocities due to the highly asymmetric stress field. Provisions are also made to account for the reactor coolant temperature and chemical composition effects. The model performance is demonstrated by a numerical example considering the crack propagation data from D4 steam generators during a 15 months operational cycle as recorded by subsequent non-destructive tube examinations.

1 INTRODUCTION

Aging of steam generator tubes made of Inconel 600 has received broad attention amongst the scientific and engineering community during recent years. In particular, stress corrosion cracking in the residual stress-dominated, tube-expansion transition zone has been extensively studied.[1,2] Following the knowledge gained by research, a plugging strategy based on a crack length criterion has been proposed and is being implemented.[3] As a consequence, steam generators affected by stress corrosion cracking have been allowed to operate with through-wall axial cracks up to a certain predefined *allowable* crack length.

In order to assess the safety implications of the crack length based plugging strategy, a probabilistic fracture mechanics model has been proposed[4] to estimate the tube failure (rupture) probabilities. Research already performed proved the applicability of probabilistic fracture mechanics and first- and second-order reliability methods (FORM and SORM).[5] Crack propagation was described in terms of a random variable whose properties were derived from the analysis of non-destructive examination records. The sensitivity studies performed showed that the uncertainty in the crack propagation predictions had the most pronounced influence on the tube failure probability.[5]

Crack propagation models already developed—a brief review is given in Section 3.1—are based either on statistical analysis of non-destructive examination results or on empirical descriptions of crack tip loading, such as

* A short version of this paper has been presented at the 12th SMiRT Conference in Stuttgart, Germany, 15–20 August 1993. It is printed in Proceedings, Vol. C/D, pp. 435–40.

strain rate or stress intensity factors. Furthermore, virtually no effort has been devoted to the investigation of the scatter intrinsic to the residual and operational stress fields, which strongly affects the crack tip loading.

In this paper an extended crack propagation model is proposed. Residual stresses due to tube manufacturing are considered as a major crack driving force, combined with operational stresses where appropriate.

A non-linear finite element analysis of the residual stress field was performed as the basis for crack propagation modelling and is presented in Section 2. The description of stresses also includes operational stresses and the variations of residual stresses due to the scatter of some influential parameters. The variation of residual stresses is modelled utilizing the response surface approach which is suggested also for subsequent reliability analysis.[6]

In Section 3 the crack propagation model based on linear-elastic fracture mechanics is proposed. It takes into account independent crack tip propagation in an asymmetrical stress field, influenced by the reactor coolant temperature and its chemical composition within the range of normal operation.

A numerical example considering specific data relating to Slovenian Krško nuclear power plant is analyzed in Section 4. The results obtained show variations of stress intensity factors caused by the residual stress field. The crack growth through 15 months long operational cycle is studied for different initial crack lengths. Reasonable agreement with data collected during in-service inspections was obtained.

2 STRESSES IN STEAM GENERATOR TUBES

The study addresses residual and operational stresses perpendicular to the axial cracks. Regarding residual stresses, only those introduced by the mechanical expansion of tubes are considered.

2.1 Residual stresses

A non-linear finite element analysis was performed to evaluate the residual stresses in a one-step rolled tube to tube-sheet joint. An axisymmetrical model was developed. Large deformations, strain-hardening effects and friction in surfaces coming into contact were taken into account according to possibilities of the ABAQUS[7] code (see Fig. 1 and Table I). Two meshes of different refinements were analyzed in order to control discretization errors. The fine mesh is shown in Fig. 1.

The calculated distribution of the residual stresses against tube length at both tube surfaces is shown in Fig. 2, together with a profile of the inside tube surface after the expansion. The area with the tensile residual hoop stress is confined at the inside surface in the tube expansion transition zone between 0 and 6 mm of tube length. The through-the-thickness residual stress distributions in axial and hoop directions are shown in Fig. 3. In Fig. 3 the tube length origin coincides with the last contact point between the tube and the expansion tool (Fig. 1).

The results obtained are qualitatively in good agreement with similar published cases.[8] Based on comparison of finite element simulation results with experimentally obtained values,[9] residual hoop stresses are considered adequate while the axial residual stresses are considered overestimated. This is acceptable for analysis which is restricted to axial cracks.

2.2 Operational stresses

Operational stresses in steam generator tubes are induced by the pressure difference between the primary and secondary loop and the thermal loading. In the vicinity of the tube sheet, the heat

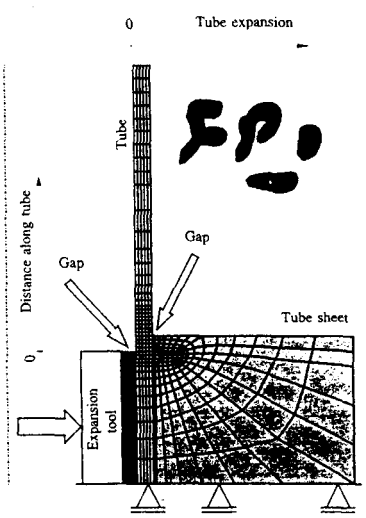

Fig. 1. Finite element model of tube to tube-sheet joint.

Table 1. Material properties used in the analysis

Property	Tube (Material—Inconel 600)	Tube-sheet (Material—Steel SA504)
Youngs modulus [GPa]	200	192
Poisson ratio [–]	0·3	0·3
Yield strength [MPa]	see Table 2	345
Strain hardening coefficient [GPa]†	3·0	2·88

† Bi-linear material; von Mises yield function; associated flow rule; isotropic strain hardening.

transfer through the tubes may be disturbed by the presence of sludge. Poor heat transfer through the tubes means vanishing temperature gradients and negligible thermal stresses.[6]

The operational stresses were determined by loading the tube with known residual stresses by an adequate pressure difference and thermal loading to obtain total (residual and operational) stresses. The distribution of the total stresses is shown in Fig. 4 together with a crack found during destructive inspection of a tube.[10] The stress contours agree very well with the crack shape. This observation is considered to support the results of stress analysis.

No additional plastic deformation was observed in the analysis of total stresses, which allows for the superposition of residual and operational stresses. Also, the operational stresses obtained as the difference between total and residual stresses agreed very well with closed form solutions for the long tube, which are well known in the theory of elasticity.

Fully developed thermal stresses tend to reduce the tensile stress at the tube inner surface and are beneficial with respect to the crack propagation. Therefore, in crack propagation calculations the operational hoop stress σ_ϕ is assumed to be induced only by the pressure difference Δp:

$$\sigma_\phi = \Delta p\left(\frac{R}{t} - \frac{1}{2}\right) \tag{1}$$

where R is the mean radius of the tube and t the tube wall thickness.

2.3 Parameters influencing the residual stress field

To characterize the residual stresses one has to:

- Identify parameters influencing the residual stress field, and
- Predict a stress field which can be used for calculation of stress intensity factors.

The stress on the inside surface of the tube is assumed to be representative for modelling the propagation of through-wall cracks. The following discussion therefore applies to the scatter of the residual hoop stresses at the inside surface of the tube.

Magnitudes and distributions of residual stresses in the expanded tube depend mostly on the tube yield stress, the initial tube to tube-sheet

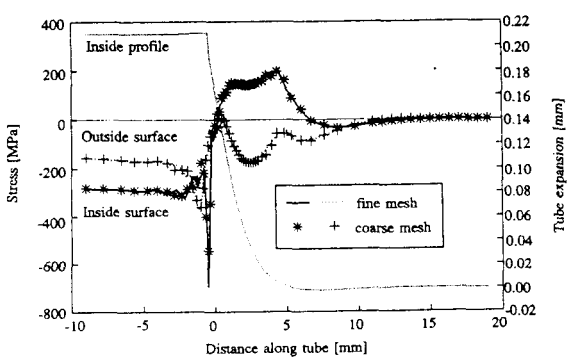

Fig. 2. Residual hoop stress distribution.

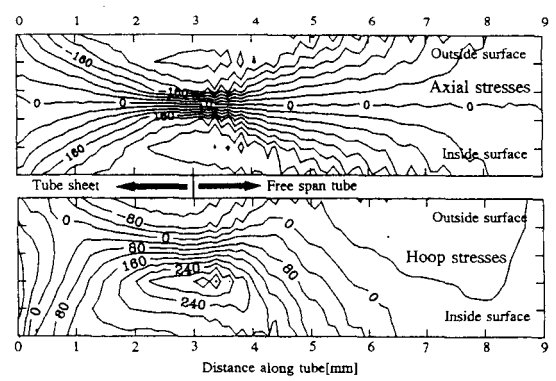

Fig. 3. Comparison of axial and hoop residual stresses across the tube wall thickness.

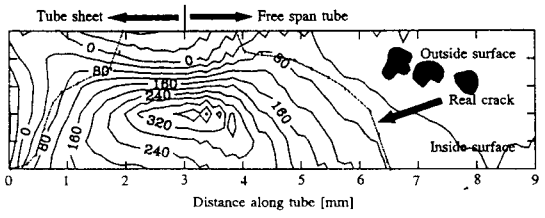

Fig. 4. Real crack in the total (residual and operational) stress field for the case with sludge.

clearance and the tube wall thickness. This has been shown for a hydraulically expanded tube by Middlebrooks *et al.*[11] It is assumed that this also applies to the mechanical tube expansion considered in this study. Ranges of selected influencing parameters are shown in Table 2.

The finite element method employed in the analysis of residual stresses can only provide a finite number of solutions at selected discrete values of influencing parameters. The number of selected points analyzed depends strongly on computational costs, which very often restrict the number of calculations to about 10. To obtain a reasonably accurate solution for any possible combination of the continuous influencing parameters, an interpolation technique has to be introduced. The response surface method is used for this purpose.

The response surface technique is designed to obtain a second-order approximation from a limited number of experiments. It requires a two step analysis.[12] First, a plan of numerical experiments called experimental design has to be defined. A variety of different experimental designs is available to fit the particular requirements. An orthogonal central composite experimental design was used in this analysis.

Results of numerical experiments performed in each point specified by the experimental design are fitted using a multidimensional regression analysis in the second step. In our case 15 analyses were required to fit a second-order hyper-surface to a response to three independent influencing parameters. Of course the validity of the response surface is restricted to the range of influencing variables analyzed (Table 2).

Table 2. Parameters influencing residual stresses

Parameter	Minimum	Nominal	Maximum
Tube yield strength (MPa)	257	362	457
Tube wall thickness (mm)	0·986	1·092	1·216
Tube to tube-sheet clearance (mm)	0·080	0·197	0·313

A cubical spline interpolation has been implemented to smooth the stress osciallations along the tube length (ABAQUS results, Fig. 5). The approximate splined curves are shown in Fig. 5 together with scatter of the residual stresses as calculated by ABAQUS[7] due to the variations in the tube yield strength. This simplification has been necessary to obtain smooth second-order derivatives of the stress intensity factors which are required by the reliability analysis.[6] The error introduced by this simplification at the crack propagation level was comparable to the errors in numerical integration of eqn (5) caused by the oscillations in the stress results (Fig. 5).

Variations in the tube yield strength mostly cause changes in the mangitude of residual stress, while variations of the initial tube to tube-sheet clearance and tube wall thickness change the position of the peak residual stress. This observation has been used to split the residual stress response in two independent variables: stress peak magnitude and its position. Both of them retained the dependency on all three influencing parameters. However, the peak stress magnitude was used to define crack tip loadings. The peak position was employed to define the crack initiation location.

3 THE CRACK PROPAGATION MODEL

3.1 Review of crack propagation models

Stress corrosion cracking of the Inconel 600 steam generator tubing has been addressed extensively in the literature.[2,13–16] Three kinds of concepts have been adopted, described below.

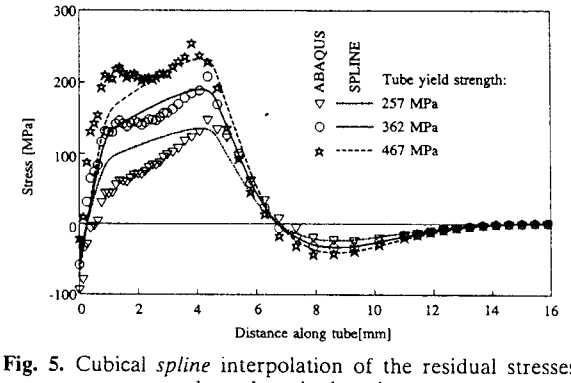

Fig. 5. Cubical *spline* interpolation of the residual stresses along the tube length.

3.1.1 Film-rupture model

This kind of modelling assumes that the local strain rate at the crack tip determines the frequency of oxide film form and rupture, thus determining the crack tip velocity. It was initially developed for sensitized stainless steels and applied also to Inconel-600.[13–15] This very general approach makes use of mechanical and electrochemical parameters governing the crack propagation. However, it has the major drawback that it is difficult to estimate the local strain rate; this was solved by introducing an empirical relation between the local strain rate and the stress intensity factor.[13]

3.1.2 Statistical analysis of non-destructive examination data

The majority of the work in this area has been done by Hernalsteen,[2] who studied behaviour of Belgian steam generators. Also, some specific studies have been made to characterize the degradation rate of Krško steam generators.[17] At the moment statistical analysis gives the most accurate crack propagation predictions, provided that the loading conditions are unchanged and the time interval between consecutive inspections is fixed during the periods analyzed. In other words, such models are not able to describe different crack growth times and plant loading histories.

3.1.3 Linear elastic fracture mechanics

Applicable linear elastic fracture mechanics models have been published by Scott[16] and, to some extent, by Pitner *et al.*[18] Scott assumed that the cracks propagate only in the direction out of the tube sheet. Furthermore, residual stresses were assumed to follow an analytical curve. Minimal and maximal residual stress values were assumed leading to two different crack growth responses. The calculation procedure of the stress intensity factor was not explained in this paper. Pitner *et al.*[18] simply fitted the function describing the dependence of stress intensity factor on the crack length. Again, only out-of-tube-sheet crack propagation was assumed. As can be deduced from the rather general paper,[18] this was done without taking into account the scatter of the residual stress field.

3.1.4 Availability of crack velocity data

The available crack tip velocity data was reviewed by Rebak *et al.*[19] and Cassagne *et al.*[20] The reported range (water temperature 330°C) is shown in Fig. 6 including the correlations used by Scott.[16] The large scatter in reported crack tip velocities is attributed to difficulties in controlling experimental parameters such as crack initiation time and crack tip loading.[20]

As a rough guide the stress intensity threshold value has been estimated[19] at 5–10 MPa $m^{1/2}$, the plateau crack tip velocity at 3×10^{-10} m s^{-1} (9·5 mm $year^{-1}$) in cold-worked tubes and 5×10^{-11} m s^{-1} (1·57 mm $year^{-1}$) in annealed tubes.[20] The influence of the reactor coolant chemical composition is considered negligible within the range expected during normal operation.[19]

3.1.5 Closure

Based on above considerations, linear elastic fracture mechanics was chosen to model the crack propagation in this study.

3.2 Crack propagation model

Cracks are assumed to initiate at the point on the internal tube surface with the maximum residual hoop stress which is located slightly above the tube sheet (Fig. 5; Tube length ≈ 4·5 mm). From this point on each crack tip propagates in the axial direction under different loading and in material with different degree of cold-working. This results in different crack tip velocities. Denoting the crack tips by $_{\pm a}$ (see Fig. 7) a modified Paris law was utilized to describe asymmetric crack propagation:

$$\dot{a}_{\pm a} = \left.\frac{da}{dt}\right|_{\pm a} = C_{\pm a}(K_{\pm a} - K_{\mathrm{ISCC}})^m \qquad (2)$$

where $C_{\pm a}$ and m are material dependent constants. K_{ISCC} represents the threshold of stress intensity factor K (see eqn (6)). A simple

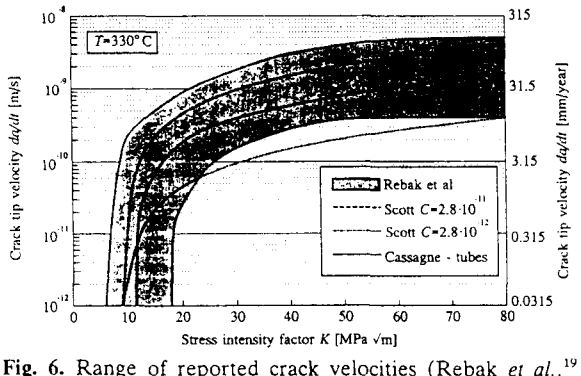

Fig. 6. Range of reported crack velocities (Rebak *et al.*,[19] Cassagne[20] and Scott[16])

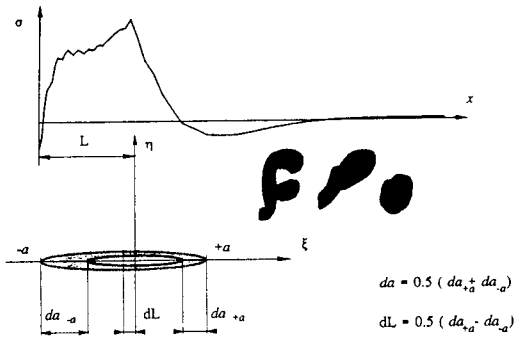

Fig. 7. The position of the crack in the residual stress field.

relationship has been established to account for different crack tip velocities in cold-worked (C_{-a}) and virgin (C_{+a}) material:

$$C_{+a} = \frac{1}{\rho} C_{-a} \tag{3}$$

The best results were obtained by setting $\rho = 2$, which is consistent with experimental data suggesting $\rho \leq 6$.[20] An Arrhenius type relation may be used to account for different temperatures T:

$$\dot{a} \propto \exp\left(\frac{-Q_{app}}{RT}\right) \tag{4}$$

The reported apparent activation energies Q_{app} are considered to be in order of 110 kJ kmol.[21] R is the gas constant (8·31 J mol^{-1}).

3.2.1 Stress intensity factor

In this study, a through-wall crack is assumed in the tube expansion transition zone above the tube sheet, loaded by an equivalent stress constant through the wall thickness. This is consistent with available non-destructive examination data.[2] Furthermore, assuming the total (residual and operational) stresses to be distributed along the tube length as $\sigma(x)$, the stress intensity factor becomes a function of crack half-length a and the crack center position L (Fig. 7). Using the Greens functions and an appropriate bulging factor:[22]

$$m(a) = 0{\cdot}614 + 0{\cdot}386 \exp\left(\frac{-2{\cdot}25a}{\sqrt{Rt}}\right) + 0{\cdot}688\left(\frac{a}{\sqrt{Rt}}\right) \tag{5}$$

the K values at both crack tips are obtained as:[23]

$$K_{\pm a} = \frac{m(a)}{\sqrt{\pi a}} \int_{-a}^{+a} \sigma(\xi + L) \sqrt{\frac{a \pm \xi}{a \mp \xi}}\, d\xi \tag{6}$$

3.2.2 Motion of the crack in the stress field

Stress intensities and hence the crack propagation may be different for the left and right crack tip (see eqn (6)). This causes a continuous change in the location of the crack center L and therefore influences the value of $K_{\pm a}$. To account for this, the propagation law (eqn (2)) was extended to a system of differential equations of the form (see also Fig. 7):

$$\dot{a} = \tfrac{1}{2}(\dot{a}_{+a} + \dot{a}_{-a}) = \tfrac{1}{2} C_{-a} \left[\frac{1}{\rho}(K_{+a} - K_{ISCC})^m + (K_{-a} - K_{ISCC})^m\right] \tag{7}$$

$$\dot{L} = \tfrac{1}{2}(\dot{a}_{+a} - \dot{a}_{-a}) = \tfrac{1}{2} C_{-a} \left[\frac{1}{\rho}(K_{+a} - K_{ISCC})^m - (K_{-a} - K_{ISCC})^m\right] \tag{8}$$

4 NUMERICAL EXAMPLE

The relevant geometry and material properties used in the analysis represent steam generators installed in Slovenian Krško Nuclear Power Plant.[4] The plant is assumed to operate at full power ($\Delta p = 63{\cdot}4$ bar) for 13 months in a 15 month inspection cycle.

4.1 Stress intensity factors

Stress intensity factors were evaluated numerically at nominal values of parameters according to eqn (6) for various values of crack lengths $2a$ and crack center positions L. The results are given in Fig. 8 and 9 for K_{-a} and K_{+a}, respectively. Figure 8 therefore contains the stress intensity values at the crack tip moving towards the inner side of the tube-sheet and Fig. 9 at the crack tip moving towards the free span tube. The crack is described by its center position and length. Also, the approximate position of the top of the tube-sheet is shown on both figures.

The region dominated by the residual stress is clearly seen for both K values (Fig. 8 and 9). It is actually confined between the shadowed 'no propagation' region at low L values and the free span tube at higher L values. The stress intensity field on Fig. 8 suggests that no crack tips will propagate below the $L = 0$ line.

The bold line denoted 'Expected crack center path' (Fig. 8 and 9) is in fact a plot of the function $L(a)$ for the cracks initiated at the point

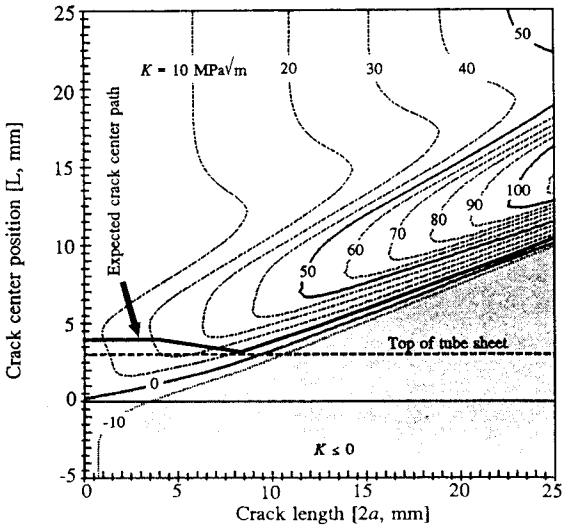

Fig. 8. Values of K_{-a} as a function of crack center position and length.

with the highest residual hoop stress. For example, following curve $L(a)$ in Fig. 8, the values of K_{-a} may be obtained given the crack length $2a$ (e.g. $2a = 1$ mm, $K_{-a} = 10$ MPa m$^{1/2}$; $2a = 4$ and 7 mm, $K_{-a} = 20$ MPa m$^{1/2}$; $2a > 8$ mm, $K_{-a} = K_{ISCC} = 9$ MPa m$^{1/2}$). Thus, curves $L(a)$ may be used to explain the behaviour of the crack in the K field. For the lower $(-a)$ crack tip, the K value falls below the K_{ISCC} values at the crack length of approximately 8 mm, where the lower crack tip arrests. This also means that under assumed conditions, no lower crack tip will

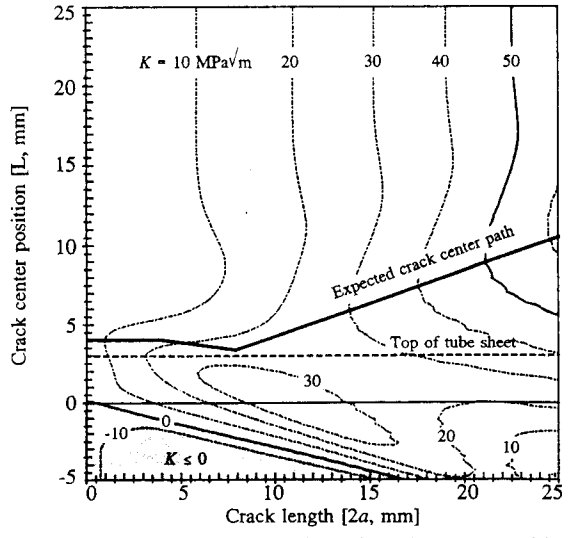

Fig. 9. Values of k_{+a} as a function of crack center position and length.

experience the very large K values shown in Fig. 8 ($K > 40$ MPa m$^{1/2}$).

Similar reasoning for the upper crack tip shows that after the lower crack tip has been arrested the upper crack tip starts to move into the region of highest K values possible at a given crack length. This indicates that the residual stress influence may be significantly reduced by crack growth, but also never completely lost.

4.2 Motion of the crack in the stress field

Figure 10 compares the calculated and observed crack center path. The calculated crack center path is sensitive to the difference between the crack tip velocities in the cold-worked (C_{-a}) and virgin (C_{+a}) tube. Observed crack center positions were obtained from the non-destructive examination results in the following way: records were grouped to classes according to measured crack lengths (e.g. 4·0 mm $< 2a \leq$ 5·0 mm). The average and standard deviations of the crack centre positions were then calculated for each class and plotted at the mean value of the class (e.g. 4·5 mm). The agreement of model predictions with the observed data is considered good taking into account possible errors in measured crack lengths (up to ±2 mm).

4.3 Crack propagation

Crack growth has been studied as a function of the initial crack length.[2] Also, the upper and lower bounds of the influence parameters derived from the specification limits have been accounted for in addition to the nominal values. This also includes the uncertainty margins for the crack growth law parameters (eqn (2); Table 3).

Predictions of the proposed model are

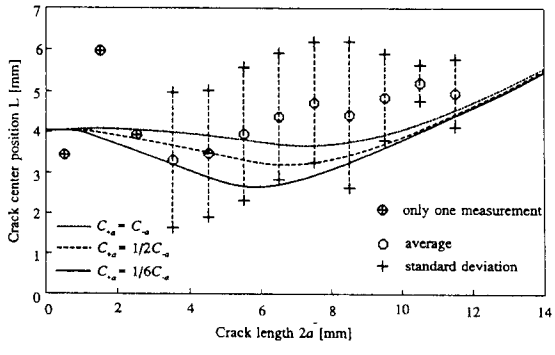

Fig. 10. Predicted and observed crack center path.

Table 3. Crack growth parameters

Parameter (at 330°C)	Minimum	Nominal	Maximum
C_{-a} ($\times 10^{-11}$)	2·5	2·8	3·1
K_{ISCC} (MPa m$^{1/2}$)	8	9	10
m	1·07	1·16	1·25

compared with maximal values observed by non-destructive examination (Fig. 11). Considering the limited non-destructive examination accuracy which affects both observed crack lengths and propagation, the agreement obtained is quite good.

Following Fig. 11, the residual stresses dominate the crack propagation up to the crack length of 8 mm. For longer cracks, the operational stresses dominate the propagation. The growth rate for cracks exceeding an initial length of 12 mm increases rather fast. This has been expected because following the modified Paris law (eqn (2)), the crack tip velocity monotonically increases with increasing stress intensity factor and, in an approximately uniform operational stress field, with increasing initial crack length.

Based on the comparison of model results with non-destructive examination crack propagation observations, the model is considered adequate. However, new experimental data on the crack velocity may significantly improve its accuracy and studies of through-the-thickness propagation.

5 CONCLUSIONS

A linear elastic fracture mechanics based model describing the propagation of axial stress-corrosion cracks in Inconel 600 steam generator tubes has been proposed. All cracks are assumed to be through-wall. The major crack driving forces considered are residual and operational stresses. Residual stresses are obtained by a non-linear-finite element simulation of the tube to tube-sheet rolling process. Asymmetric crack propagation is taken into consideration which is caused by large residual stress gradients and different amounts of cold-work along the crack path which strongly influence the crack tip velocity.

A numerical example was chosen to represent the operational conditions of a real steam generators as closely as possible. The fields of stress intensity factors are given separately for both crack tips. Also, the crack motion in the stress field is studied in some detail. The crack propagation predictions obtained showed good agreement with non-destructive examination results of cracks.

The model presented in this paper was developed to be used in reliability analysis of the cracked steam generator tubes. This required two additional features: (1) analysis of the changes in the residual stress field caused by the uncertainty in influence parameters and (2) smooth second-order derivatives of the stress intensity factors with respect to the influence parameters of the residual stress field. A second-order response surface was developed for this purpose.

Improving the accuracy of the proposed model and introducing through-the thickness crack propagation are considered the main future topics. However, they depend heavily on the availability and accuracy of experimental crack tip velocity data.

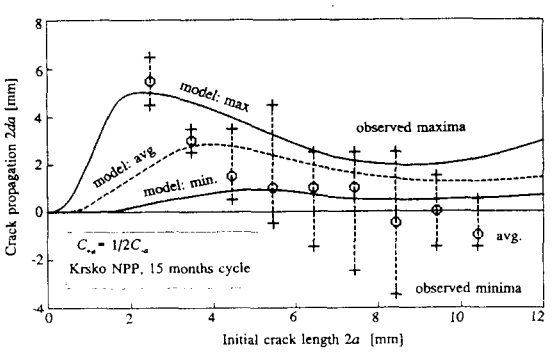

Fig. 11. Predicted and observed crack growth (c_{-a} = 1/2C_{-a}).

ACKNOWLEDGEMENTS

Financial support from the Ministry of Science and Technology of Republic of Slovenia and the International Office of KFA Jülich, Germany, is gratefully acknowledged.

REFERENCES

1. Flesch, B. & Cochet, B., Leak-before-break in steam generator tubes. *Int. J. of Pres. Ves. and Piping*, **43** (1990) 165–79.
2. Hernalsteen, P. Prediction models for the PWSCC degradation process in tube roll transitions. NEA-CSNI-UNIPEDE Specialist Meeting on Operating Experience with Steam Generators, Brussels, Belgium (1991).

3. Van Vyve, J., Hernalsteen, P. & Mathonet, J., Steam generator tube plugging criteria. In *Trans. 1st Int. Conf. on Engineering Support to NPP Operation,* 1991.
4. Mavko, B. & Cizelj, L., Failure probability of axially cracked steam generator tubes: A probabilistic fracture mechanics model. *Nucl. Technol.* **98**(2) (1992) 171–7.
5. Cizelj, L., Mavko, B. & Riesch-Oppermann, H., Application of first- and second-order reliability methods in the safety assessment of cracked steam generator tubing. *Nucl. Engng and Design,* **147** (in press). (1994) 359-68
6. Cizelj, L., On the estimation of the Steam Generator Maintenance Efficiency by the Means of Probabilistic Fracture Mechanics (in Slovene). Dissertation, University of Ljubljana, Slovenia (1993).
7. *ABAQUS User's Manual Ver. 4.9.* Hibbit, Karlsson and Sorensen, Inc., Providence, USA.
8. Flesch, B. *et al.,* Contraintes en service et sur-contraintes de denting dans les zones de transition des generateurs de vapeur des reacteurs 900 MWe et 1300 MWe. SFEN International Symposium, Fontevraud, vol. 2 (1990) pp. 268–80.
9. Duc, M. H., Churier-Bosnec, H. & Faidy, C., Computation of stresses in French steam generator tubes. In *Trans. of 11th Conf. on SMiRT,* Vol. F, Tokyo, Japan 1991, pp. 361–70.
10. Frederick, G., Mathonet, J., Hernalsteen, P. & Dobbeni, D., *Development and Justification of New Plugging Criteria Applicable to the Cracking Phenomena in the Tubing of Steam Generators.* Belgatom, Brussels, 1989.
11. Middlebrooks, W. B., Harrod, D. L. & Gold, R. E., Residual stresses associated with the hydraulic expansion of steam generator tubing into tubesheets. In *Trans. of 11th Conf. on SMiRT,* Vol. , Tokyo, Japan, 1991, pp. 343–54.
12. Myers, R. H., *Response Surface Methodology.* Allyn & Bacon, Inc., Boston, USA, 1971.
13. Ford, F. P., Andresen, P. L., Development and use of a predictive model of crack propagation in 304/316L, A533B/A508 and Inconel 600/182 alloys in 288 C water. In *Proc. of 4th Int. Symp. on Envir. Deg. of Mater. in NPP Systems,* Traverse City, USA, 1988, pp. 789–800.
14. Garud, Y. S., Incremental damage formulation and its application to assess IGSCC growth of circumferential cracks in a tube. *Corrosion,* **47**(7) (1991) 523–7.
15. Garud, Y. S., Service stresses within the expansion transition of tubes in a PWR U-tube heat-exchanger design including local discontinuity and geometry effects. In *Trans. of 11th Conf. on SMiRT,* Vol. F, Tokyo, Japan, 1991, pp. 355–60.
16. Scott, P. M., An Analysis of Primary Water Stress Corrosion Cracking in PWR Steam Generators, NEA-CSNI-UNIPEDE Specialist Meeting on Operating Experience with Steam Generators, Brussels, Belgium, 1991.
17. Dvoršek, T., Cizelj, L. & Mavko, B., Recent experience with Krško steam generators. Paper presented at ASME/IEEE International Joint Power Generation Conference. Kansas City, Mo., USA, Paper 93-JPGC-NE-2, 17–20 October 1993.
18. Pitner, P., Riffard, T., Granger, B. & Flesch, B., Application of probabilistic fracture mechanics to optimize the maintenance of PWR steam generator tubes. *Nucl. Engng and Design,* **142** (1993) 89–100.
19. Rebak, R. B., McIlree, A. R., & Sklarska-Smialowska, Z., Effects of pH and stress intensity on crack growth rate in alloy 600 in lithiated + borated waters at high temperatures. In *Proc. of 5th Symp. on Environmental Degradation of Materials in NPP Systems,* Monterey, Ca., USA, 25–29 August 1991, pp. 511–7.
20. Cassagne, T. B., Combrade, P., Foucault, M. A. & Gelpi, A., The influence of mechanical and environmental parameters on the crack growth behaviour of alloy 600 in PWR primary water. In *Proc. of 12th Scandinavian Corrosion Congress & Eurocorr '92,* Espoo, Finland, 1992, pp. 55–67.
21. Speidel, M. O. & Magdowski, R., Stress corrosion crack growth of cold-worked nickel base alloy 600. In *Proc. of the Int. Conf. on Corrosion-Deformation-Interactions,* Fointanebleau, France, 5–7 October 1992.
22. Erdogan, F., Ductile fracture theories for pressurized pipes and containers. *Int. J. Press. Ves. & Piping,* **4** (1976) 253–83.
23. Terada, H. & Nakajima, T., Analysis of stress intensity factor of a crack approaching welding bead. *Int. J. of Fracture,* **27** (1985) 83–90.